0.1 Axial load and uniform bending

It is preliminarily noted that the elementary extensional-flexural solution is exact with respect to the Theory of Elasticity if the following conditions hold:

- beam constant section;
- beam rectilinear axis;
- absence of locally applied loads;
- absence of shear resultants[1] (i.e. constant bending moments);
- principal material directions of orthotropy are uniform along the section, and one of them is aligned with the beam axis;
- the ν_{31} and the ν_{32} Poisson's ratios[2] are constant along the section, where 3 means the principal direction of orthotropy aligned with the axis. Please note that $E_i\nu_{ji} = E_j\nu_{ij}$, and hence $\nu_{ji} \neq \nu_{ij}$ for a generally orthotropic material.

Most of the above conditions are in fact violated in many textbook structural calculations, thus suggesting that the elementary beam theory is robust enough to be adapted to practical applications, i.e. limited error is expected if some laxity is used in circumscribing its scope[3].

The extensional-flexural solution builds on the basis of the following simplifying assumptions:

- the in-plane[4] stress components $\sigma_x, \sigma_y, \tau_{xy}$ are null;
- the out-of-plane shear stresses τ_{yz}, τ_{zx} are also null;

[1] A locally pure shear solution may be in fact superposed; such solution may however not be available for a general cross section.

[2] We recall that ν_{ij} is the Poisson's ratio that corresponds to a contraction in direction j, being a unitary extension applied in direction i in a manner that the elastic body is subject to a uniaxial stress state.

[3] Measures for both the error and the violation have to be supplied first in order to quantify the approximation.

[4] Both the *in-plane* and the *out-of-plane* expressions for the characterization of the stress/strain components refer to the cross sectional plane.

- the axial elongation ϵ_z linearly varies along the cross section, namely

$$\epsilon_z = a + bx + cy \tag{1}$$

or, equivalently[5], each cross section is assumed to remain planar in the deformed configuration.

The three general constants a, b and c possess a physical meaning; in particular a represents the axial elongation $\bar{\epsilon}$ as measured at the centroid[6], c represents the $1/\rho_x$ curvature[7] whereas b represent the $1/\rho_y$ curvature, apart from its sign.

Figure 1 (c) justifies the equality relation $c = 1/\rho_x$; the beam axial fibers with a Δz initial length are elongated by the curvature up to a $\Delta\theta\,(\rho_x + y)$ deformed length, where $\Delta\theta\rho_x$ equates Δz based on the length of the unextended fibre at the centroid. By evaluating the axial strain value for a general fiber, it follows that $\epsilon_z = 1/\rho_x\ y$.

In addition, Figure 1 (c) relates the $1/\rho_x$ curvature to the displacement component in the local y direction, namely v, and to the section rotation angle with respect to the local x axis, namely θ, thus obtaining

$$\frac{d\theta}{dz} = \frac{1}{\rho_x}, \quad \theta = -\frac{dv}{dz}, \quad \frac{d^2v}{dz^2} = -\frac{1}{\rho_x} \tag{2}$$

Following analogous considerations, see 1 (e), we may similarly obtain

$$\frac{d\phi}{dz} = \frac{1}{\rho_y}, \quad \phi = +\frac{du}{dz}, \quad \frac{d^2u}{dz^2} = +\frac{1}{\rho_y} \tag{3}$$

where ϕ is the cross section rotation about the local y axis, and u is the x displacement component.

According to the assumptions in the preamble, a uniaxial stress state is assumed, where the only nonzero σ_z stress component may be determined as

$$\sigma_z = E_z\epsilon_z = E_z\left(\bar{\epsilon} - \frac{1}{\rho_y}x + \frac{1}{\rho_x}y\right) \tag{4}$$

[5]The axial, out-of-plane displacement $\Delta w = \int_{\Delta l}\epsilon_z dz = \Delta_l\,(a + bx + cy)$ accumulated between two contiguous cross sections with an Δl initial distance, is consistent with that of a relative rigid body motion.

[6]or, equivalently, the average elongation along the section, in an integral sense.

[7]namely the inverse of the beam curvature radii as observed with a line of sight aligned with the x axis. Curvature is assumed positive if the associated θ section rotation grows with increasing z, i.e. $d\theta/dz > 0$.

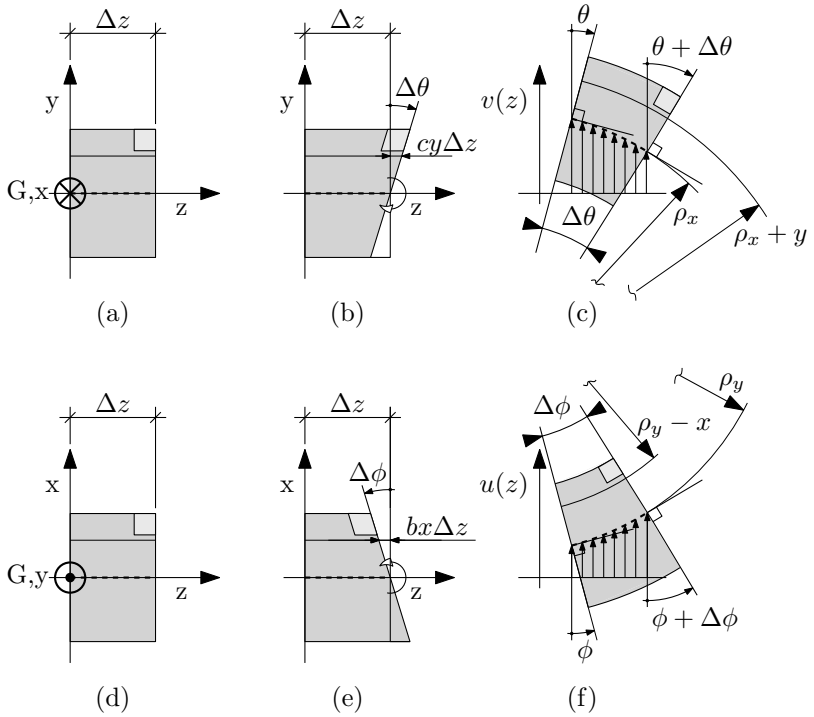

Figure 1: A differential fibre elongation proportional to the y coordinate induces a curvature $1/\rho_x$ on the normal plane with respect to the x axis. A differential fibre contraction proportional to the x coordinate induces a curvature $1/\rho_y$ on the normal plane with respect to the y axis. The didascalic trapezoidal deformation modes (b) and (e) clearly associate the differential elongation/contraction with the positive relative end rotation; they are however affected by a spurious shear deformation as evidenced by the skewed corner.

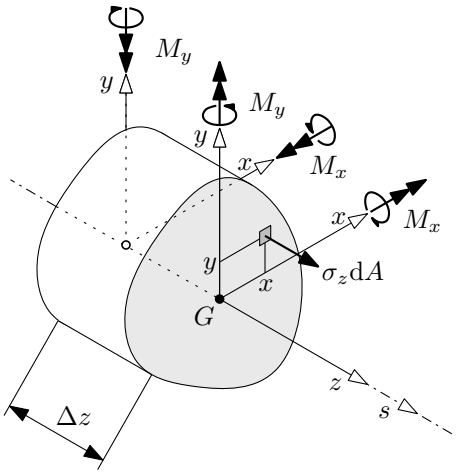

Figure 2: Positive x and y bending moment components adopt the same direction of the associated local axes at the beam segment end showing an outward-oriented arclength coordinate axis; at beam segment ends characterized by an inward-oriented local z axis, the same positive bending moment components are locally counter-oriented to the respective axes.

Stress resultants may easily be evaluated based on Fig. 2 as

$$N = \iint_A E_z \epsilon_z dA = \overline{EA}\bar{\epsilon} \tag{5}$$

$$M_x = \iint_A E_z \epsilon_z y dA = \overline{EJ}_{xx}\frac{1}{\rho_x} - \overline{EJ}_{xy}\frac{1}{\rho_y} \tag{6}$$

$$M_y = -\iint_A E_z \epsilon_z x dA = -\overline{EJ}_{xy}\frac{1}{\rho_x} + \overline{EJ}_{yy}\frac{1}{\rho_y} \tag{7}$$

where the combined material/cross-section stiffness moduli

$$\overline{EA} = \iint_A E_z(x,y)\ dA \tag{8}$$

$$\overline{EJ}_{xx} = \iint_A E_z(x,y) yy\ dA \tag{9}$$

$$\overline{EJ}_{xy} = \iint_A E_z(x,y) yx\ dA \tag{10}$$

$$\overline{EJ}_{yy} = \iint_A E_z(x,y) xx\ dA \tag{11}$$

may also be rationalized as the cross section area and moment of inertia, respectively, multiplied by a suitably averaged Young modulus, evaluated in the axial direction.

Those moduli simplify to their usual $E_z A, E_z J_{**}$ analogues, where the influence of the material and of the geometry are separated if the former is homogeneous along the beam cross section.

From Eqn. 5 we obtain

$$\bar{\epsilon} = \frac{N}{\overline{EA}}. \tag{12}$$

By concurrently solving Eqns. 6 and 7 with respect to the $1/\rho_x$ and $1/\rho_y$ curvatures, we obtain

$$\frac{1}{\rho_x} = \frac{M_x\overline{EJ}_{yy} + M_y\overline{EJ}_{xy}}{\overline{EJ}_{xx}\overline{EJ}_{yy} - \overline{EJ}_{xy}^2} \tag{13}$$

$$\frac{1}{\rho_y} = \frac{M_x\overline{EJ}_{xy} + M_y\overline{EJ}_{xx}}{\overline{EJ}_{xx}\overline{EJ}_{yy} - \overline{EJ}_{xy}^2} \tag{14}$$

$$\frac{1}{\rho_{\text{eq}}} = \sqrt{\frac{1}{\rho_x^2} + \frac{1}{\rho_y^2}} \tag{15}$$

Axial strain and stress components may then be obtained for any cross section point by substituting the above calculated generalized strain components $\bar{\epsilon}$, $1/\rho_x$ and $1/\rho_y$ holding for the extensional-flexural beam into Eqn. 4.

As an alternative, the following

thus obtaining

$$\sigma_z = E_z \epsilon_z \tag{16}$$

$$= \alpha M_x + \beta M_y + \gamma N \tag{17}$$

where

$$\alpha\left(x, y, E_z, \overline{EJ}_{**}\right) = E_z(x,y)\frac{-\overline{EJ}_{xy}x + \overline{EJ}_{yy}y}{\overline{EJ}_{xx}\overline{EJ}_{yy} - \overline{EJ}_{xy}^2} \tag{18}$$

$$\beta\left(x, y, E_z, \overline{EJ}_{**}\right) = E_z(x,y)\frac{-\overline{EJ}_{xx}x + \overline{EJ}_{xy}y}{\overline{EJ}_{xx}\overline{EJ}_{yy} - \overline{EJ}_{xy}^2} \tag{19}$$

$$\gamma\left(x, y, E_z, \overline{EA}\right) = E_z(x,y)\frac{1}{\overline{EA}}. \tag{20}$$

The peak axial strain is obtained at points farther from neutral axis of the stretched section; such neutral axis may be graphically defined as follows:

- the coordinate pair

$$(x_N, y_N) \equiv \left(\frac{\bar{e}\rho_x^2\rho_y}{\rho_x^2+\rho_y^2}, -\frac{\bar{e}\rho_x\rho_y^2}{\rho_x^2+\rho_y^2}\right);$$

  defines its nearest pass-through point with respect to the G centroid; the two points coincide in the case $\bar{\epsilon} = 0$.

- its orientation is defined by the unit vector

$$\hat{n}_{\parallel} = \sqrt{\rho_x^2+\rho_y^2}\left(\frac{1}{\rho_x}, \frac{1}{\rho_y}\right),$$

  whereas the direction

$$\hat{n}_{\perp} = \sqrt{\rho_x^2+\rho_y^2}\left(-\frac{1}{\rho_y}, \frac{1}{\rho_x}\right),$$

  is orthogonal to the neutral axis, and oriented towards growing axial elongations.

The cross section projection on the $(N, \hat{n}_\perp)$ line defines a segment whose ends are extremal with respect to the axial strain.

If the bending moment and the curvature component vectors are imposed to be parallel, i.e.

$$\lambda \begin{bmatrix} M_x \\ M_y \end{bmatrix} = \begin{bmatrix} \frac{1}{\rho_x} \\ \frac{1}{\rho_y} \end{bmatrix} = \underbrace{\frac{1}{\overline{EJ}_{xx}\overline{EJ}_{yy} - \overline{EJ}_{xy}^2} \begin{bmatrix} \overline{EJ}_{yy} & \overline{EJ}_{xy} \\ \overline{EJ}_{xy} & \overline{EJ}_{xx} \end{bmatrix}}_{[\overline{EJ}]} \begin{bmatrix} M_x \\ M_y \end{bmatrix} \tag{21}$$

an eigenpair problem is defined that leads to the definition of the principal directions for the cross sectional bending stiffness. In particolar, the eigenvectors of the $[\overline{EJ}]$ matrix define the two principal bending stiffness directions, and the associated $\overline{EJ}_{11}, \overline{EJ}_{22}$ eigenvalues constitute the associated bending stiffness moduli.

TODO: please elaborate...

0.2 Stresses due to the shear cross section resultants

In the presence of nonzero shear resultants, the bending moment exhibits a linear variation with the axial coordinate z in a straight beam. Based on the beam segment equilibrium we have

$$S_y = \frac{dM_x}{dz}, \quad S_x = -\frac{dM_y}{dz}, \tag{22}$$

as rationalized in Fig. 4, with $dz \to 0$ and M_x, M_y differentiable with respect to z.

The linear variation of the bending-induced curvature in z causes a likewise linear variation of the pointwise axial strain; stress variation is also linear in the case of constant E_z longitudinal elastic modulus.

In particular, the differentiation with respect to z of σ_z as espressed in Eqn. 17 returns

$$\frac{d\sigma_z}{dz} = \alpha\left(x, y, E_z, \overline{EJ}_{**}\right) S_y - \beta\left(x, y, E_z, \overline{EJ}_{**}\right) S_x \tag{23}$$

since its α, β, γ factors are constant with respect to z; the bending moment derivatives are here expressed in terms of the shear resultants, as in Eqns. 22.

Figure 3 rationalizes the axial equilibrium for an elementary volume of material; we have

$$\frac{d\tau_{zx}}{dx} + \frac{d\tau_{yz}}{dy} + \frac{d\sigma_z}{dz} + q_z = 0 \tag{24}$$

where, for the specific case, the distributed volumetric load q_z is zero.

It clearly emerges from such relation that the shear stresses τ_{zx}, τ_{yz}, that were null within the uniform bending framework, are non-uniform along the section – and hence not constantly zero – in the presence of shear resultants.

A treatise on the pointwise solution of a) the equilibrium equations 24, once coupled with b) the compatibility conditions and with c) the the material elastic response, is beyond the scope of the present contribution, although it has been derived for selected cross sections in e.g. [1].

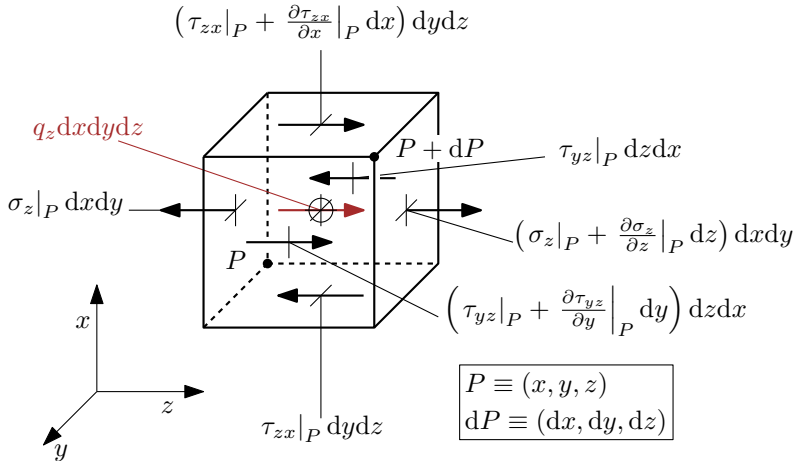

Figure 3: Equilibrium conditions with respect to the axial z translation for the infinitesimal volume extracted from the beam. In the case under scrutiny, the distributed volume action q_z is null.

0.2.1 The Jourawsky approach and its extension for a general section

The aforementioned axial equilibrium condition, whose treatise is cumbersome for the infinitesimal volume, may be more conveniently dealt with if a finite portion of the beam segment is taken into account, as in Figure 4.

A beam segment is considered whose axial extent is dz; the beam cross section is partitioned based on a (possibly curve, see Fig. 5) line that isolates an area portion A^* – and the related beam segment portion – for further scrutiny; axial equilibrium equation may then be stated for the isolated beam segment portion as follows

$$\bar{\tau}_{zi} t = \int_{A^*} \frac{d\sigma_z}{dz} dA, \tag{25}$$

where

$$\bar{\tau}_{zi} = \frac{1}{t} \int_t \tau_{zi} dr \tag{26}$$

is the average shear stress acting in the z direction along the cutting surface; i is the (locally normal) inward direction with respect to such

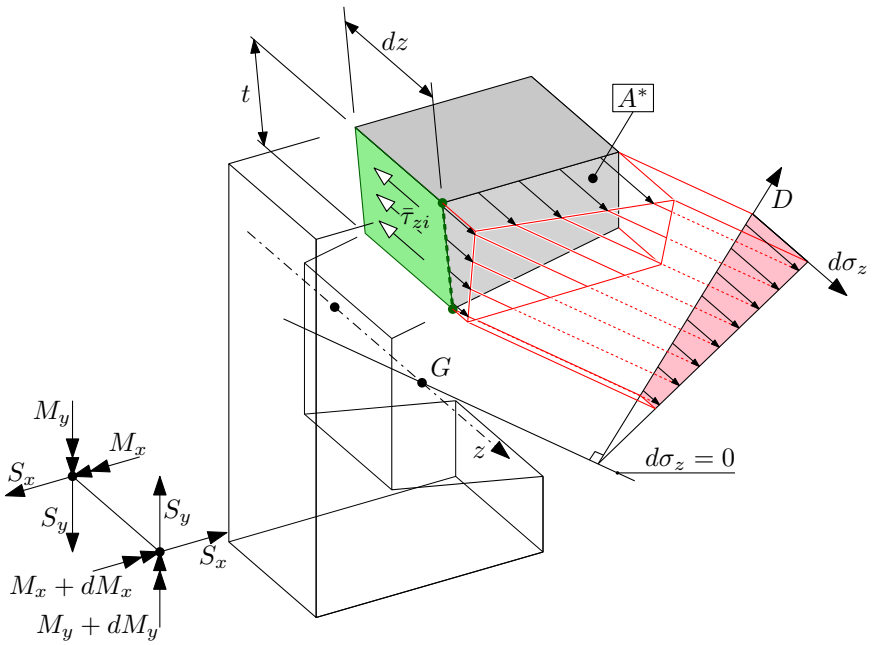

Figure 4: Equilibrium conditions for the isolated beam segment portion. It is noted that the null σ_z variation locus, $d\sigma_z = 0$, does not coincide with the bending neutral axis in general. Also, the depicted linear variation of $d\sigma_z$ with the D distance from such null $d\sigma_z$ locus does not hold in the case of non-uniform E_z modulus.

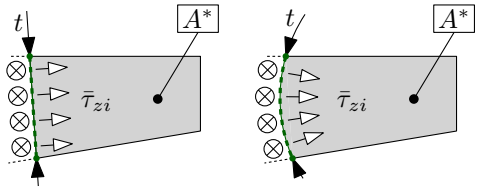

Figure 5: The curve employed for isolating the beam segment portion defines the direction of the τ_{zi} components whose average value is evaluated.

a surface. Due to the reciprocal nature of the shear stresses, the same $\bar{\tau}_{zi}$ shear stress acts along the cross sectional plane, and locally at the cutting curve itself. These shear actions are assumed positive if inward directed with respect to A^*.

The $\bar{\tau}_{zi}t$ product is named *shear flow*, and may be evaluated along a general cutting curve.

It is noted that, according to Eqn. 25, no information is provided with regard to a) the τ_{zr} shear stress that acts parallel to the cutting curve, nor b) the pointwise variation of τ_{zi} with respect of its average value $\bar{\tau}_{zi}$. If the resorting to more cumbersome calculation frameworks is not an option, those quantities are usually just neglected; an informed choice for the cutting curve is thus critical for a reliable application of the method.

In the simplified case of a) uniform material and b) local x, y axes that are principal axes of inertia (i.e. $J_{xy} = 0$), the usual formula is obtained

$$\bar{\tau}_{zi}t = \int_{A^*} \left(\frac{yS_y}{J_{xx}} + \frac{xS_x}{J_{yy}} \right) dA = \frac{\bar{y}^* A^*}{J_{xx}} S_y + \frac{\bar{x}^* A^*}{J_{yy}} S_x, \tag{27}$$

where $\bar{y}^* A^*$ and $\bar{x}^* A^*$ are the first order area moments of the A^* section portion with respect to the x and y axes, respectively[8].

0.2.2 Shear induced stresses in an open section, thin walled beam

In the case of thin walled profiles, the integral along the isolated area in Eqn. 25 may be performed with respect to the arclength coordinate alone; the value the $d\sigma_z/dz$ integrand assumes at the wall midplane is supposed representative of its integral average along the wall thickness, thus obtaining

$$\bar{\tau}_{zi}t = q_{zi} = \int_0^s \int_{-t/2}^{t/2} \frac{d\sigma_z}{dz} dr d\varsigma \approx \int_0^s \left. \frac{d\sigma_z}{dz} \right|_{r=0} t d\varsigma. \tag{28}$$

Such assumed equivalence strictly holds for a) straight wall segments[9] and b) a linear variation of the integrand along the wall, a

[8] According to the employed notation, $(\bar{x}^*, \bar{y}^*)$ are the centre of gravity coordinates for the A^* area.

[9] i.e. the Jacobian of the $(s, r) \mapsto (x, y)$ mapping is constant with r.

condition, the latter, that holds if the material properties are homogeneous with respect to the wall midplane[10]; in the more general case, the error incurred by this approach vanishes with vanishing thickness for what concerns assumption a), whereas if the material is inhomogeneous, through-thickness averaged $\bar{E}_z, \bar{G}_{zi}$ moduli may be employed in place of their pointwise counterpart.

If a thin walled section segment is considered such that it is not possible to infer that the interfacial shear stress is zero at at least one of its extremities, a further term needs to be considered for the equilibrium, thus obtaining

$$\bar{\tau}_{zi}(s)t(s) = q(s) = \int_a^s \frac{d\sigma_z}{dz} t d\varsigma + \underbrace{\bar{\tau}_{zi}(a)t(a)}_{q_A}. \tag{29}$$

In the case of open thin walled profiles, however, such a choice for the isolated section portion is suboptimal, unless the q_A term is known.

0.2.3 Shear induced stresses in an closed section, thin walled beam

In the case of a closed thin walled, generally asymmetric section, the search for a point along the wall at which the shear flow may be assumed zero is normally not viable, and the employment of Eq. 29 in place of the simpler Eq. 28 is unavoidable.

In this case, a parametric value for the $\bar{\tau}_{iz}$ shear stress is assumed for a set of points along the cross section midcurve – one for each elementary closed loop[11] if the points are non-redundantly chosen[12].

In the multicellular cross section example shown in Figure 6, two elementary loops are detected; shear flows at the A, B points are parametrically defined as $\tau_A t_A$ and $\tau_B t_B$, respectively.

The $\tau(s)$ shear stress at each point along the profile wall may then be determined based on Eqn. 29 as a function a) of the shear resultant

[10] a linear $d\epsilon_z/dz$ axial strain variation is in fact associated to the curvature variation in z, and not an axial stress variation;

[11] i.e. a closed loop not enclosing any other closed loop.

[12] Redundancy may be pointed out by ideally cutting the cross section at these points: if a monolithic open cross section is obtained, the point choice is not redundant; if a portion of the section is completely isolated, and a loop remains closed, the location of these points causes redundancy.

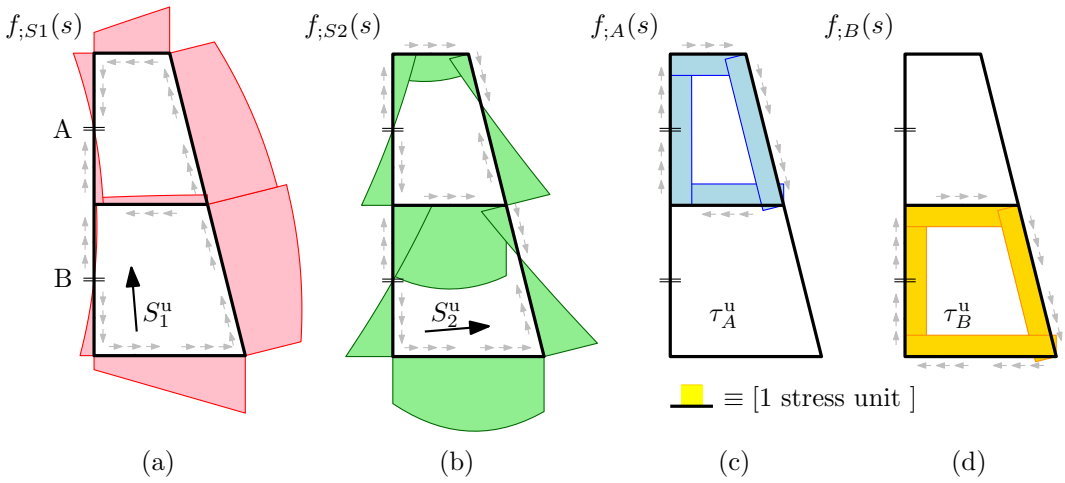

Figure 6: Contributions to the $\tau_{zi}(s)$ shear stress along the profile walls associated to a) a unit shear force component S_1^{u} applied along the first principal axis of inertia, whose magnitude equals the product of the cross section area and the unit stress, b) an analogous shear force component S_2^{u} aligned with the second principal axis of inertia, c) a unit shear stress τ_A^{u} applied at the opposite fictitious cut surfaces at A, and d) a unit shear stress τ_B^{u} applied at the opposite fictitious cut surfaces at B. Profile wall thickness is constant in the presented example, thus producing a continuous shear stress diagram, whereas continuity is rather aa unit shear stress τ_A^{u} applied at the opposite fictitious cut surfaces at a property of the shear flow.

components S_x and S_y, and b) of the parametrically defined shear stresses at the A,B points.

Due to the assumed linear response for the profile, superposition principle may be employed in isolating the four elementary contributions to the shear stress flow along the section.

The first two elementary contributions $f_{;Sx}(s)$ and $f_{;Sy}(s)$ are respectively due to the action alone of the x and y shear force components, whose magnitudes S_x^{u} and S_y^{u} is assumed equal the product of the stress unit (e.g. 1 MPa) and of the cross sectional area. Those forces are assumed to act in the ideal absence of shear flow at points where the latter is assumed as a parameter (points A and B in Figure 6).

Since the condition of zero shear flow is stress-compatible with an opening in the closed section loop, the cross section may be idealized as severed at the assumed shear flow points, and hence open. The equilibrium-based solution procedure derived for the open thin-walled section may hence be profitably applied.

A family of further elementary contributions, one for each of the assumed shear stress points, may be derived by imposing zero parametric shear flow at all the points but the one under scrutiny, and in the absence of externally applied shear resultants. The elastic problem may be rationalized as an open – initially closed, then ideally severed – thin walled profile, that is loaded by an internal constraint action whose magnitude is unity in terms of stresses. Equilibrium considerations reduce to the conservation of the shear flow due to the absence of $d\sigma_z/dz$ differential axial stress, as in the case of a closed profile under torsion discussed below.

Figures 6 (a) and (b) show the shear stress contributions $f_{;S1}(s)$ and $f_{;S2}(s)$ induced in the ideally opened (i.e. zero redundant shear flows at the A,B points) multicellar profile by the first and the second shear force components, respectively; due to the author distraction, such figure refers to shear components aligned with the principal directions of bending stiffness, and not to the usual x,y axes.

Figures 6 (c) and (d) show the shear stress contributions $f_{;A}(s)$ and $f_{;B}(s)$ associated to unity values for the parametric shear flows at the A, B segmentation points, respectively.

The cumulative shear stress distribution for the section in Figure 6

is

$$\tau(s) = \frac{S_1}{\mathcal{A}} f_{;S1}(s) + \frac{S_2}{\mathcal{A}} f_{;S2}(s) + \tau_A f_{;A}(s) + \tau_B f_{;B}(s) \tag{30}$$

where s is a suitable arclength coordinate.

The associated elastic potential energy may then be integrated over a Δz beam axial portion, thus obtaining

$$\Delta U = \int_s \frac{\tau^2}{2G_{sz}} t \Delta z ds \tag{31}$$

According to the Castigliano second theorem, the ΔU derivative with respect to the $\bar{\tau}_i$ assumed shear stress value at the i-th segmentation point equates the generalized displacement with respect to which the internal constraint reaction works, i.e. the $t\Delta z\bar{\delta}_i$ integral of the relative longitudinal displacement between the cut surfaces; we hence have

$$\frac{\partial \Delta U}{\partial \bar{\tau}_i} = \bar{\delta}_i t \Delta z \tag{32}$$

The $\bar{\delta}_i$ symbol refers to the average value along the $t\Delta z$ area of such axial relative displacement.

Material continuity requires zero $\bar{\delta}_i$ value at each segmentation point, thus defining a set of equations, one for each $\bar{\tau}_i$ unknown parameter, whose solution leads to the definition of the actual shear stress distribution along the closed wall profile.

Bibliography

[1] A. E. H. Love, *A treatise on the mathematical theory of elasticity.* Cambridge university press, 2013.